Int. J. Heat Mass Transfer. Vol. 19, pp. 589–596. Pergamon Press 1976. Printed in Great Britain

A STUDY OF TWO LIMITING CASES IN CONVECTIVE AND RADIATIVE HEAT TRANSFER WITH NONGRAY GASES

D. R. JENG,* E. J. LEE and K. J. DEWITT
Departments of Mechanical* and Chemical Engineering, University of Toledo, Toledo, OH 43606, U.S.A.

(*Received* 22 *November* 1974 *and in revised form* 5 *December* 1975)

Abstract—A study is made for two optical limits in a convective and radiative heat-transfer process for nongray gases flowing in a circular tube having a constant uniform wall temperature. The governing energy equations which are valid for the optically thin and the large path length limits are obtained for fully developed laminar flow with a non-black wall. Numerical results for the temperature profiles, local conductive, radiative and total heat fluxes are obtained and the validity of these limiting cases is discussed.

NOMENCLATURE

A_i, total band absorptance [cm^{-1}];
A_{0i}, correlation quantity [cm^{-1}];
$\bar{A}_i$, dimensionless total band absorptance, A_i/A_{0i};
C_p, specific heat at constant pressure [cal/g °K];
e_ω, Planck's function [cal/(h cm^2)/cm^{-1}];
k, thermal conductivity [cal/cm h °K];
Nu, Nusselt number;
P, gas pressure [atm];
q^c, conductive heat flux [cal/(cm^2 h)];
q^R, radiative heat flux [cal/(cm^2 h)];
q^T, total heat flux, $= q^c + q^R$ [cal/(cm^2 h)];
Q^c, dimensionless conductive heat flux, $-q^c R/kT_w$;
Q^R, dimensionless radiative heat flux, $-q^R R/kT_w$;
Q^T, dimensionless total heat flux, $-R(q^c+q^R)/kT_w$;
r, radial coordinate [cm];
R, radius of the tube [cm];
T, temperature [°K];
T_b, bulk temperature [°K];
u_i, dimensionless coordinate $C_{0i}^2 Pr$;
u_{0i}, dimensionless path length $C_{0i}^2 PR$;
u_0, $\sum_{i=1}^{I} u_{0i}$;
v, velocity in x direction [cm/s];
v_m, mean velocity in x direction [cm/s];
x, axial coordinate [cm].

Greek symbols

α, angle;
α_ω, spectral absorptivity;
β, angle;
ε, surface emittance;
η, dimensionless coordinate, $r/R = u_i/u_{0i}$;
θ, dimensionless temperature, $1 - T/T_w$;
θ_b, dimensionless bulk temperature, $1 - T_b/T_w$;
κ_ω, absorption coefficient of wave number ω [cm^{-1}];
μ, $\cos\alpha$;
ρ, density [g/cm^3];
τ, optical thickness.

Subscripts

cl, value at centerline;
i, ith band;
w, value at wall;
ω, wave number.

INTRODUCTION

THE STUDY of simultaneous convective and radiative heat transfer in a cylindrical geometry has become increasingly important due to recent interest in heat-transfer calculations involving many high temperature systems, such as modern propulsion systems, plasmas, power plants, etc., where most of the flow geometries we are dealing with are cylindrical. Landram *et al.* [1] have investigated the heat transfer in turbulent pipe flow with optically thin radiation subjected to a constant wall heat flux. Later, the same subject was re-examined experimentally and theoretically by Habib and Greif [2] without the restriction to optically thin gases. In a previous paper [3], we have investigated the heat transfer in the fully developed laminar flow of gray and nongray radiating gases in a cylindrical tube having a uniform wall temperature for a wide range of optical thickness. Two methods were employed for solving the energy equation in [3]. The first method was to expand the dimensionless temperature function, θ^4, appearing in the radiative flux into a Taylor series, retaining only the first three terms. This procedure makes it possible to reduce the energy equation from a non-linear integrodifferential equation to a non-linear differential equation which was in turn solved numerically by an iterative procedure. The second method was an integral method with a linearized approximation (this approximation is valid only if the temperature variation throughout the system is small). In both methods, it was found that the required numerical calculation was quite tedious. The purpose of the present paper is to investigate two limiting cases in which simple approximations can be introduced for the radiative term in the energy equation. For the purpose of establishing the limits of validity and the accuracy of these limiting formulations, comparisons will be made with the results obtained in [3]. The particular gases considered for this work are carbon monoxide, carbon dioxide, water vapor and methane.

FORMULATION OF THE PROBLEM

The physical model and coordinate system used in the present study is illustrated in Fig. 1. Let's consider an absorbing and emitting, but non-scattering gas having a fully developed velocity profile in a circular tube. The tube walls may be black or gray, and are considered to have isothermal, diffuse reflectors and emitters. The flow is steady, and the gas is assumed to be an isotropic, homogenous medium in local thermodynamic equilibrium, which can absorb and emit thermal radiation in a diffuse manner. A radiation field in an absorbing medium definitely affects the motion and the temperature distribution. This is due to the presence of a radiation pressure, a radiation energy density, and a radiation heat flux. For temperature levels utilized in this work, the radiation pressure and energy density are negligible compared with the molecular momentum flux and the molecular energy density, respectively. Therefore, the effect of the radiation heat flux is the only contribution from the thermal radiation. Under the assumption that the fluid has constant transport properties and constant density, the energy equation in integral form for the nongray gas with fully developed laminar flow has been derived and is given in [3, 4]. For the convenience of the reader, they are reproduced below.

$$\eta\frac{\partial\theta}{\partial\eta}+2Nu\int_0^{\eta}(\eta'-\eta'^3)\theta(\eta')\,d\eta'$$
$$=\frac{4R}{\pi k}\sum_{i=0}^{l}A_{0i}u_{0i}\left(\frac{de_{\omega i}}{dT}\right)_{T_w}\int_0^{\sin^{-1}\eta}\cos\beta\,d\beta$$
$$\times\left\{\int_{\sin\beta}^{\eta}\frac{\eta'\,d\eta'}{F(\eta',\beta)}\theta\int_{\alpha=0}^{\pi/2}\cos\alpha\,\bar{A}_i'\left[\frac{u_{0i}\zeta^{\eta,\beta}_{\eta',\beta}}{\cos\alpha}\right]d\alpha\right.$$
$$-\int_{\eta}^{1}\frac{\eta'\,d\eta'}{F(\eta',\beta)}\theta\int_{\alpha=0}^{\pi/2}\cos\alpha\,\bar{A}_i'\left[\frac{u_{0i}\zeta^{\eta',\beta}_{\eta,\beta}}{\cos\alpha}\right]d\alpha$$
$$+\int_{\sin\beta}^{1}\frac{\eta'\,d\eta'}{F(\eta',\beta)}\theta\int_{\alpha=0}^{\pi/2}\cos\alpha\,\bar{A}_i'\left[\frac{u_{0i}\zeta^{\eta',\beta}_{\eta,\beta}}{\cos\alpha}\right]d\alpha$$
$$+\frac{4}{\pi}(1-\varepsilon_i)^{m+1}\int_{\beta'=0}^{\pi/2}\cos\beta'\int_{\sin\beta'}^{1}\frac{\eta'}{F(\eta',\beta')}$$
$$\left.\times\theta\,.\,B(\eta,\beta,\eta',\beta')\,d\eta'\,d\beta'\right\}\quad(1)$$

where

$$B(\eta,\beta,\eta',\beta')=\int_{\alpha'=0}^{\pi/2}\int_{\alpha=0}^{\pi/2}\cos\alpha'\cos^2\alpha$$
$$\times\left\{\bar{A}_i'\left[u_{0i}\left(\frac{\zeta^{1,\beta'}_{\eta',\beta'}}{\cos\alpha'}+\frac{\zeta^{1,\beta}_{\eta,\beta}}{\cos\alpha}+1{\cdot}16m\right)\right]\right.$$
$$+\bar{A}_i'\left[u_{0i}\left(\frac{\zeta^{1,\beta'}_{\eta',\beta'}}{\cos\alpha'}+\frac{\zeta^{1,\beta}_{\eta,\beta}}{\cos\alpha}+1{\cdot}16m\right)\right]$$
$$-\bar{A}_i'\left[u_{0i}\left(\frac{\zeta^{1,\beta'}_{\eta',\beta'}}{\cos\alpha'}+\frac{\zeta^{1,\beta}_{\eta,\beta}}{\cos\alpha}+1{\cdot}16m\right)\right]$$
$$\left.-\bar{A}_i'\left[u_{0i}\left(\frac{\zeta^{1,\beta'}_{\eta',\beta'}}{\cos\alpha'}+\frac{\zeta^{1,\beta}_{\eta,\beta}}{\cos\alpha}+1{\cdot}16m\right)\right]\right\}$$
$$\times d\alpha'\,d\alpha.$$

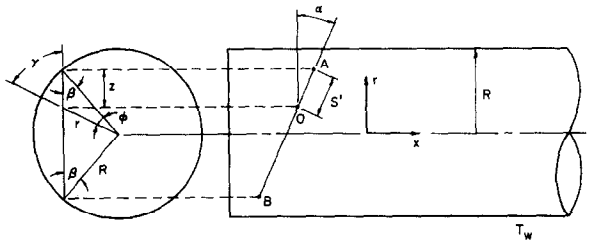

FIG. 1. Physical model and coordinate system.

In the above, $\bar{A}_i'(y)$ is the derivative of $\bar{A}_i(y)$ with respect to y and

$$F(\eta,\beta)=(\eta^2-\sin^2\beta)^{1/2}$$
$$\zeta^{\eta,\beta}_{\eta',\beta}=F(\eta,\beta)-F(\eta',\beta),\qquad \zeta^{\eta',\beta}_{\eta,\beta}=F(\eta',\beta)-F(\eta,\beta)$$
$$\zeta^{\eta',\beta}_{\eta,\beta}=F(\eta',\beta)+F(\eta,\beta),\qquad \zeta^{1,\beta'}_{\eta',\beta'}=F(1,\beta')+F(\eta',\beta')$$
$$\zeta^{1,\beta}_{\eta,\beta}=F(1,\beta)+F(\eta,\beta)\ldots\text{etc.}$$

and the Nusselt number based on the total heat-transfer rate is defined as:

$$Nu=\frac{hD}{k}=-\frac{2Rq_w^T(x)}{kT_w\theta_b}\quad(2)$$

where $q_w^T(x)$ is the total heat flux at the wall to be determined. It is worthwhile to state the assumptions and to summarize the procedure used in the derivation of (1). Equation (1) has been derived for the thermally fully developed case. This statement means that the dimensionless temperature profile, $(T_w-T)/(T_w-T_b)$, is invariant with x. Furthermore, the total radiation flux, the right hand side of (1), is obtained by integrating the spectral radiative flux, equation (5) of [3], over the band width $\Delta\omega_i$:

$$q_i^R=\int_{\Delta\omega_i}q_{\omega i}^R\,d\omega\quad\text{for the } i\text{th band, and}\quad q^R=\sum_{i=1}^{l}q_i^R$$

where l is the number of bands. In the integration of q_i^R, it is often convenient to use the total band absorptance A_i, which is defined as the integral of the spectral absorptivity, α_ω, over the width of the band, $\Delta\omega_i$, in the following manner:

$$A_i(y)=\int_{\Delta\omega_i}\alpha_\omega\,d\omega=\int_{\Delta\omega_i}[1-\exp(-\kappa_\omega y)]\,d\omega.\quad(3)$$

The function A may be expressed by the exponential band model [5] as

$$A_i=A_{0i}\ln\left\{u_i f(t_i)\left[\frac{u_i+2}{u_i+2f(t_i)}\right]+1\right\}\quad(4)$$

where

$$u_i=C_{0i}^2Pr,\quad t_i=[C_{2i}^2/(4C_{1i}C_{3i})]P_e=B_i^2P_e,$$
$$f(t_i)=2{\cdot}94[1-\exp(-2{\cdot}6t_i)].$$

The quantity B_i^2 characterizes the effect of pressure broadening, since B_i^2 is proportional to the rate of the line width to line spacing. The band width parameter, $A_{0i}=C_{3i}$, is a function of temperature only. The quantity t_i is the line structure parameter, and P_e is the effective broadening pressure, given by

$$P_e=[(P_k+bP_a)/P_0]^n,\quad P_0=1\text{ atm}$$

where P_a is the absorbing gas partial pressure, P_k is the broadening gas partial pressure, and b is the self-broadening power of the a-molecule with respect to the k-molecule. The pressure parameter, n, which is always less than or equal to unity, accounts for the partial overlapping of bands with different lower states. The quantities b and n are estimated experimentally by using various gas compositions. The values of the correlation quantities C_{1i}, C_{2i}, C_{3i}, A_{0i}, C_{0i}^2 and B_i^2, for several gases are available in the literature [6].

In equation (1), we have also linearized the radiative flux equation by a restriction of moderately small temperature differences within the gas. The Planck function, $e_{\omega i}(T)$, may therefore be written as

$$e_{\omega i}(T) \simeq e_{\omega}(T_w) + \left(\frac{\mathrm{d}e_{\omega i}}{\mathrm{d}T}\right)_{T_w}(T - T_w).$$

The numerical solutions of equation (1) for wide range of optical thickness were carried out and reported in [3]. In this paper, a study is presented on the two limiting cases in this heat-transfer problem. These two cases represent the optically thin and the large path length limit.

OPTICALLY THIN LIMIT

For small u_{0i}, i.e. $u_{0i} \ll 1$, $\bar{A}_i(u_i) = u_i$, $\bar{A}_i' = 1$, the optical thin form of the energy equation becomes

$$\eta\frac{\partial\theta}{\partial\eta} + 2Nu\int_0^{\eta}(\eta' - \eta'^3)\theta(\eta')\,\mathrm{d}\eta' = \frac{8}{\pi}N\int_0^{\sin^{-1}\eta}\cos\beta\,\mathrm{d}\beta \times \int_{\sin\beta}^{\eta}\frac{\theta(\eta')\eta'\,\mathrm{d}\eta'}{F(\eta',\beta)} \quad (5)$$

$$N = \frac{PR^2}{k}\sum_{i=1}^{l} A_{0i}C_{0i}^2\left(\frac{\mathrm{d}e_{\omega i}}{\mathrm{d}T}\right)_{T_w}. \quad (6)$$

It readily follows that the dimensionless parameter, N, characterizes the relative importance of radiation vs conduction within the gas. For particular values of P and R, it is actually the dimensionless gas property

$$\frac{N}{PR^2} = \frac{1}{k}\sum_{i=1}^{l} A_{0i}C_{0i}^2\left(\frac{\mathrm{d}e_{\omega i}}{\mathrm{d}T}\right)_{T_w} \quad (7)$$

which denotes the relative importance of radiation to conduction. It should be emphasized that this quantity characterizes the radiation–conduction interaction only in the optically thin limit.

It should also be noted here that, under optically thin conditions, the effect of surface emittance upon the radiative transfer vanishes. Under optically thin conditions the photon mean free path is much larger than the characteristic physical dimension. Correspondingly, photons emitted by a given fluid element will travel directly to the bounding surfaces, and any intervening absorption of photons by the fluid will be negligible. Therefore, the surface radiosity is evaluated as if the gas were completely transparent, and since this corresponds to an isothermal enclosure for the present problem, the surface radiosity is equal to the black radiation irrespective of the value of the surface emissivity.

Equation (5) does not appear to possess a closed form solution even with simplification. Thus a numerical solution has been obtained by assuming a temperature profile of the form

$$\theta(\eta) = \sum_{n=0}^{M'} a_{2n}\eta^{2n}.$$

Such a profile can be made to satisfy $M'+1$ conditions in order to determine the unspecified constants a_{2n}'s. With this form of the temperature profile, the boundary condition at $\eta = 0$ is automatically satisfied, but that at the wall may be written as the equation:

$$\sum_{n=0}^{M'} a_{2n} = 0.$$

In addition, M' more conditions can be imposed. Probably the simplest procedure is to satisfy equation (5) at M' discrete points, η_i. The values of η_i were chosen as equally spaced points from the center of the tube to the wall, excluding the point at the wall. The specification of the centerline or bulk temperature is also required. This procedure is then followed by the iteration scheme. A value of the Nusselt number is assumed and the a_{2n}'s are then found by the above mentioned procedure. With the resultant temperature profile, the total heat flux at the wall and the Nusselt number are recalculated by equation (2). This procedure will be repeated until the assumed Nusselt number and the recalculated Nusselt number are matched within the difference of 10^{-4}.

Numerical solutions of equation (5) for the optically thin approximation are illustrated in Fig. 2 for a range of the radiation–conduction interaction parameter N.

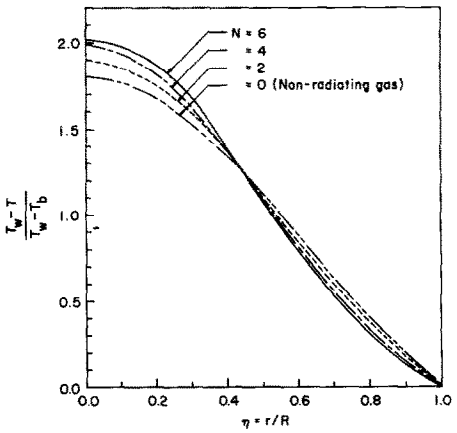

FIG. 2. Effect of parameter N on temperature profile for optically thin limit.

The fully developed temperature profile, $(T_w - T)/(T_w - T_b)$ has been chosen as one of the coordinates in Fig. 2, so that the profile is invariant with axial direction. Furthermore, with N as a parameter, the temperature profile for the optical thin limit will not depend on the type of gas. The quantity N for individual gases may be obtained by equation (6) using the correlation quantities, which are available in the literature for several gases [6]. For purposes of comparison, the temperature distribution for non-radiating gas has also been included. It is seen that the temperature field

departs more and more from that of the pure conduction and convection case as the parameter N increases. If one plots T/T_w vs η, the temperature profile will increase with increasing N. This is physically justifiable, since increasing N can be interpreted as increasing the heat transfer from the wall to the gas due to the radiation contribution, and the resulting profile departs more from that for conduction and convection alone.

The local variation of conductive, radiative, and the sum of both energy fluxes has been plotted for selected values of parameters in Fig. 3. Inspection of the figure reveals that when the parameter N increases, only the change of the radiative heat flux becomes significant,

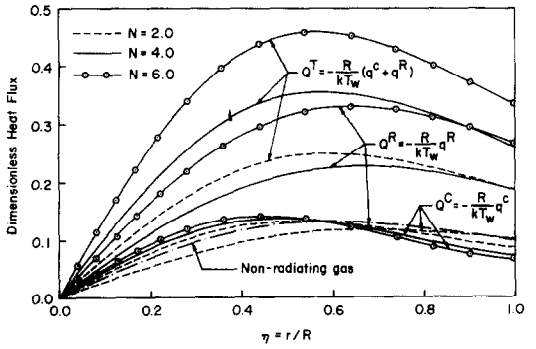

FIG. 3. Variation of local conductive, radiative, and total heat fluxes with dimensionless radius for optically thin limit, $T_{cl}/T_w = 0.9$.

with very little change occurring in the conductive flux. In the vicinity of the tube wall, the conductive flux for the radiating gases is less than that of non-radiating gas and the conductive flux decreases with increasing N. This implies that the temperature gradient in the vicinity of the wall decreases with increasing N and this trend holds up to $\eta \sim 0{\cdot}6$. For $\eta < 0{\cdot}6$, the above statement reverses.

It is of interest to compare the temperature and heat-transfer results predicted from the optically thin approximation with those obtained by the band absorptance model, equation (1), and to consider a range of the optical thickness, u_0, over which to apply the optically thin approximation. The heat-transfer results obtained by equation (1) are compared with those from the optically thin approximation in Table 1 for CO and in Table 2 for CH_4 and H_2O. As seen from Table 1, the difference in the quantities listed between the optical thin approximation and the band absorptance solution for $u_0 = 2{\cdot}27$ is quite large. Thus, the optically thin approximation is not suitable for this condition. However, for $u_0 = 0{\cdot}114$, i.e. for $u_0 \ll 1$, agreement between the two results is very good, and this again confirms the criterion required to apply this approximation. For CH_4 and H_2O, the optical thicknesses of which are 0·41 and 0·26, respectively, the agreement between the two results in both cases is good, being within a maximum error of 1·07 per cent, except for Q_w^R where there are discrepancies of 10 per cent for H_2O with $u_0 = 0{\cdot}26$ and 69 per cent for CH_4 with $u_0 = 0{\cdot}41$. The results of Tables 1 and 2 also illustrate that either a lower pressure or a shorter tube radius could be chosen to apply the optically thin approximation at a fixed wall temperature.

Table 1. Comparison of results for CO (2-bands): $T_w = 1140\,^\circ\text{K}$, $T_{cl} = 1060\,^\circ\text{K}$

	$P = 1$ atm $R = 2{\cdot}54$ cm		$P = 0{\cdot}1$ atm $R = 1{\cdot}27$ cm	
	Optically thin approx. (5)	Band model (1)	Optically thin approx. (5)	Band model (1)
θ_{Tb}	0·035 0 *(0·039 0)	0·038 0	0·038 8 (0·039)	0·038 9
Q_w^R	0·135 7 (0·0)	0·042 7	0·003 9 (0·0)	0·0039
Q_w^C	0·053 8 (0·071)	0·071 2	0·070 6 (0·071)	0·071 1
Q_w^T	0·189 5 (0·071)	0·113 9	0·074 5 (0·071)	0·075 0
Nu	10·817 (3·657)	5·996	3·840 (3·657)	3·866
u_0	2·27	2·27	0·114	0·114
N	4·142		0·104	

*Numbers in the parenthesis indicate the values for pure conduction and convection.

Table 2. Comparison of results for CH_4 (2-bands) and H_2O (5-bands): $P = 0{\cdot}3$ atm, $R = 0{\cdot}635$ cm, $\Delta T = 100\,^\circ\text{K}$

	CH_4 (2-bands)		H_2O (5-bands)	
	Optically thin approx. (5)	Band model (1)	Optically thin approx. (5)	Band model (1)
$T_w(^\circ\text{K})$	750	750	1050	1050
θ_{Tb}	0·073 8 *(0·074 0)	0·073 9	0·052 7 (0·052 8)	0·052 7
Q_w^R	0·004 4 (0·0)	0·002 6	0·005 3 (0·0)	0·004 8
Q_w^C	0·134 6 (0·135 2)	0·135 0	0·095 9 (0·096 6)	0·096 0
Q_w^T	0·139 (0·135 2)	0·137 6	0·101 2 (0·096 6)	0·100 8
Nu	3·766 (3·657)	3·726	3·840 (3·657)	3·826
u_0	0·41	0·41	0·26	0·26
N	0·062		0·104	

*Numbers in the parenthesis indicate the values for pure conduction and convection.

It is also seen that under the optically thin limit, the interaction parameter N is very small. In other words, conduction dominates over radiation as a heat-transfer mechanism, and thus the resulting temperature profile is close to that for pure conduction and convection. The optically thin approximation also predicts a smaller gradient and a larger radiative flux than that obtained by the band absorptance solution at the wall. In general, it also predicts a slightly lower mean temperature.

As discussed above, there certainly exists a condition for the optically thin limit for some gases in the physical

system considered here, and for such a system under this limit the optically thin approximation is expected to predict reasonably accurate heat-transfer results. In summary, it is recommended that for engineering applications, the optically thin approximation, equation (5), may be used for the calculation of heat transfer when $u_0 < 0{\cdot}4$, but to obtain a radiative heat flux within an accuracy of 10 per cent, $u_0 < 0{\cdot}25$ is recommended.

THE LARGE PATH LENGTH LIMIT

The conventional optically thick (or Rosseland) limit does not apply to infrared gaseous radiation. The reason for this is that the rotational line intensity approaches zero asymptotically in the band wings, such that regardless of the physical dimensions, there will be optically non-thick radiation occurring in the band wings. In other words, the band wings will constitute regions for which there will be a continuous transition from opaque to the transparent limit.

For vibration–rotation bands, even though the Rosseland equation is inapplicable, a large path length limit does exist and is achieved when $u_{0i} \gg 1$ for each band of importance. In this limit $\bar{A}_i(u_i) = \ln(u_i)$ and $\bar{A}_i'(u_i) = 1/u_i$ such that their substitution in equation (1) gives

$$\eta\frac{\partial\theta}{\partial\eta} + 2Nu\int_0^{\eta}(\eta'-\eta'^3)\theta\,d\eta' = M\int_0^{\sin^{-1}\eta}\cos\beta\,d\beta\left\{\int_{\sin\beta}^{1}\left[\frac{1}{\zeta^{\eta,\beta}_{\eta',\beta}}+\frac{1}{\zeta^{\eta',\beta}_{\eta,\beta}}\right]\frac{\theta\eta'\,d\eta'}{F(\eta'\beta)} + \frac{16}{\pi^2}\sum_{m=0}^{\infty}(1-\varepsilon)^{m+1}\times\int_{\beta'=0}^{\pi/2}\cos\beta'\int_{\sin\beta'}^{1}\frac{\eta'\,d\eta'}{F(\eta',\beta')}\times\theta B_2\,d\eta'\,d\beta'\right\} \quad (8)$$

where

$$B_2(\eta,\beta,\eta',\beta') = \int_{\alpha'=0}^{\pi/2}\int_{\alpha=0}^{\pi/2}\cos\alpha'\cos^2\alpha \times\left\{\left[\frac{\zeta^{1,\beta'}_{\eta',\beta'}}{\cos\alpha'}+\frac{\zeta^{1,\beta}_{\eta,\beta}}{\cos\alpha}+1{\cdot}16m\right]^{-1} + \left[\frac{\zeta^{1,\beta'}_{-\eta',\beta'}}{\cos\alpha'}+\frac{\zeta^{1,\beta}_{+\eta,\beta}}{\cos\alpha}+1{\cdot}16m\right]^{-1} - \left[\frac{\zeta^{1,\beta'}_{\eta',\beta'}}{\cos\alpha}+\frac{\zeta^{1,\beta}_{-\eta,\beta}}{\cos\alpha}+1{\cdot}16m\right]^{-1} - \left[\frac{\zeta^{1,\beta'}_{-\eta',\beta'}}{\cos\alpha'}+\frac{\zeta^{1,\beta}_{-\eta,\beta}}{\cos\alpha}+1{\cdot}16m\right]^{-1}\right\}\times d\alpha'\,d\alpha$$

where

$$M = \frac{R}{k}\sum_{i=1}^{I}A_{0i}\left(\frac{de_{\omega i}}{dT}\right)_{T_w}. \quad (9)$$

The dimensionless parameter M constitutes the radiation–conduction interaction parameter for the large path length limit. Inspection of equation (8) reveals that only A_{0i} of the three correlation quantities, A_{0i}, C_{0i}^2, and B_i^2, remains through the definition of M as defined above.

The absence of the line structure quantity B_i^2 is obvious because the line structure of the band plays no role when radiative transfer occurs solely in the wings of the band. Since the individual band intensities correspond to $A_{0i}C_{0i}^2$, the absence of C_{0i}^2 illustrates that the radiative transfer process is independent of the band intensities in the large path length limit. This is physically reasonable, since the central portion of the band does not contribute to radiative transfer in this limit.

A further simplication associated with equation (8) is that the temperature profile within the gas is independent of the pressure. This is not the case with the general formulation, equation (1), for which pressure appears both in the dimensionless band path length u_{0i} and in the line structure parameter t.

Numerical solutions of equation (8) for the large path length limit have been carried out for a range of the radiation–conduction parameter, M. Since the integral on the r.h.s. of equation (8) possesses a singularity at $\eta = 1$, a temperature profile of the form

$$\theta(\eta) = \sum_{n=0}^{M'}A_{2n}\eta^{2n}(1-\eta^2)$$

has been assumed and a similar procedure as described in the previous section has been followed to obtain the numerical results. For the sake of convenience and brevity, the results are presented only for the case of a black bounding surface. It should be emphasized that the interaction parameter, M, as defined in equation (9), characterizes the relative importance of radiation vs conduction only for the large path length limit.

Figure 4 shows the effect of the interaction parameter M on the temperature distribution. When the parameter M increases, the temperature distribution departs from that of a non-radiating gas, as would be expected.

Comparison of the results between the band absorptance and the large path length limit for CO_2 and CH_4, and CO gases are shown in Figs. 5–7 for a tube radius of 2·54 cm and wall temperatures of 500, 700 and 1000 °K, respectively. In order to make the comparison more effective, we have chosen θ as one of the coordinates rather using the fully developed temperature

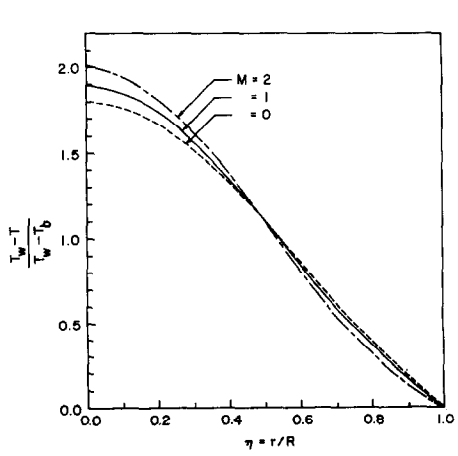

FIG. 4. Effect of parameter M on temperature profile for large path length limit, $\varepsilon = 1.0$.

profile. For these comparisons, only the increment of pressure was considered to achieve a large u_0, although the large u_0 limit can be obtained either by going to larger values of R or to higher pressure. As explained earlier, the temperature profile obtained by the large path length approximation is invariant with pressure.

For CO_2, it is seen from Fig. 5 that at a wall temperature of 500 °K, the agreement between the mean temperature results obtained by the band absorptance and the large path length limit is very good. At the

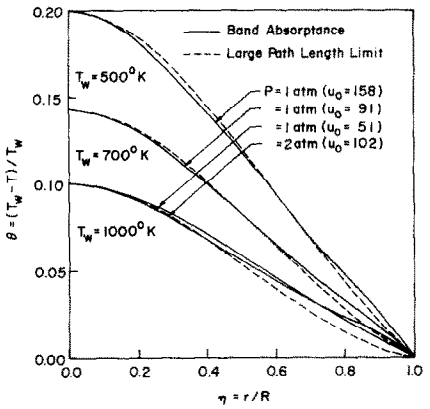

FIG. 5. Comparison of temperature profiles for CO_2 (3-bands) with $R = 2.54$ cm, $T_w - T_{cl} = 100$°K and $\varepsilon = 1.0$.

condition of 1 atm pressure shown, the optical thickness, u_0, is about 158, and it satisfies the criterion for this approximation, i.e. $u_0 \gg 1$. Even for a wall temperature of 700 °K, the agreement between the two results is good. For a wall temperature of 1000 °K, however, the difference between both the temperature distributions and the mean temperature for the two cases is appreciable at a pressure of 1 atm. As the pressure increases, the mean temperature results approach those obtained by the large u_0 limit, and it can be seen that the large length limit is essentially a limiting solution for large pressure. However, the striking feature is that the effect of pressure is to raise the temperature in the cold region and to lower the temperature in the hot region, causing the mean temperature results to approach those obtained by the large u_0 limit. It should be emphasized that the large path length limit, as treated in this work, is not an exact asymptotic limit since it makes use of the logarithmic asymptote for the band absorptance which in itself is an approximate limiting expression. Similarly, for the large path length limit, we may obtain analogous results concerning the heat-transfer process.

The corresponding results for CH_4 and CO are shown in Figs. 6 and 7, respectively, and once again they show that the large path length limit is a limiting solution for high pressures. For the case of a wall temperature at 500 °K and a pressure of 1 atm, the agreement between the two mean temperature results is very good as well as the individual temperature profile, unlike the case of CO_2.

From an evaluation of the entire results, it may be

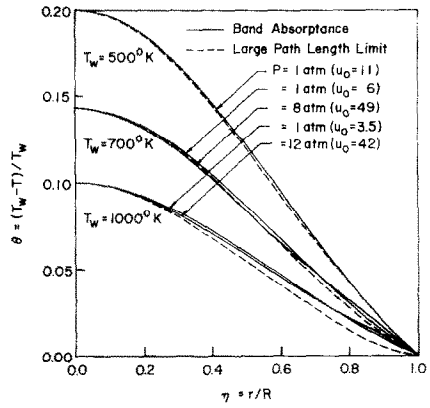

FIG. 6. Comparison of temperature profiles for CH_4 (2-bands) with $R = 2.54$ cm, $T_w - T_{cl} = 100$°K, and $\varepsilon = 1.0$.

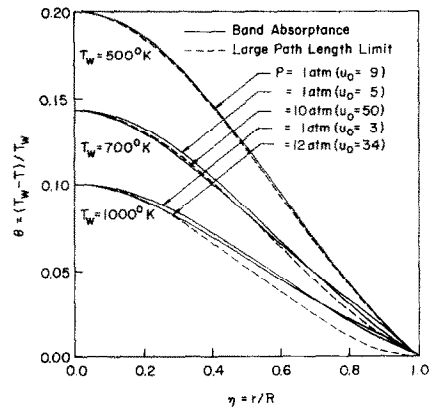

FIG. 7. Comparison of temperature profiles for CO (2-bands) with $R = 2.54$ cm, $T_w - T_{cl} = 100$°K and $\varepsilon = 1.0$.

concluded that the large path length limit constitutes an upper bound upon the influence of radiation transfer on the temperature profile within a gas. However, it should be mentioned that the range of the optical thickness to apply the large path length limit approximation is different for different gases. For instance, in the case of CO with $T_w = 700$ °K, and $P = 10$ atm, i.e. $u_0 = 50$, the result obtained by the large path length limit is good within a maximum error of 2 per cent, while for CO_2 with $T_w = 1000$ °K, $P = 1$ atm, i.e. $u_0 \simeq 51$, the result is good only within a maximum error of 9·6 per cent. For the same accuracy of the result, therefore, higher path length should be accounted for CO_2.

VARIATION OF THE CENTERLINE TEMPERATURE, BULK TEMPERATURE AND HEAT FLUX IN THE AXIAL DIRECTION

The governing differential equation (1) is valid at a specific axial position and the knowledge of the variation of centerline temperature (with assumed initial value), bulk temperature and total wall heat flux along the axial direction x is required for heat-transfer calculations to be made. To obtain this information, with assumed T_{cl} (or T_b) at a specified section x (or initial location corresponding to $x = 0$), the governing equation can be solved for θ and hence for q_w^T at that section

as described in the previous discussion. The value of T_b at the next section is then obtained by integration of the following equation:

$$\frac{dT_b}{dx} = -\frac{2q_w^T(x)}{Rv_m\rho C_p} \tag{10}$$

which is derived by making an energy balance on an elemental slice of fluid. The new T_{cl} can then be readily calculated by the fully developed criterion. In this manner, the complete solution of the governing equation can be generated. For the optically thin and large path length limits, the results are illustrated in Figs. 8 and 9, in which the dimensionless axial distance is defined as

$$\xi' = K''x \tag{11}$$

where

$$K'' = \frac{2k}{\rho C_p v_m R^2}.$$

In both cases, the centerline temperature at $\xi' = 0$ (or $x = 0$) was assumed to be 0·3.

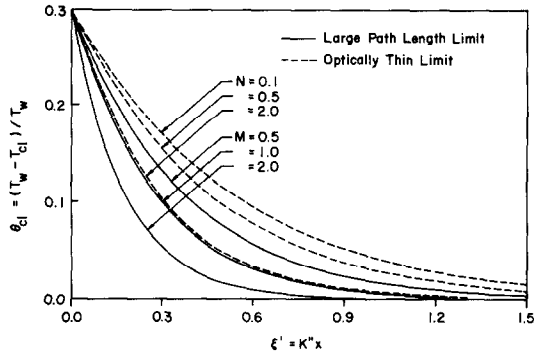

FIG. 8. Variation of centerline temperature with axial distance for optically thin and large path length limits.

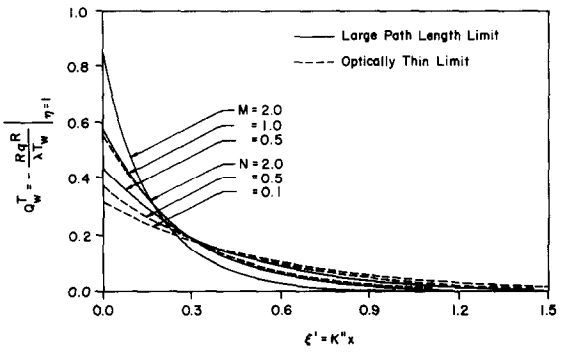

FIG. 9. Variation of total wall heat flux with axial distance for optically thin and large path length limits.

To illustrate the use of Figs. 8 and 9 and to get some information about heat transfer for a specific system, we will consider simple examples. It was shown that the optically thin approximation for CO at $P = 0{\cdot}1$ atm, $R = 1{\cdot}27$ cm, $T_{cl} = 1060\,°K$, and $T_w = 1140\,°K$, as illustrated in Table 1, predicts reasonably accurate heat-transfer results. Let's consider the same physical conditions but with the different centerline temperature of $T_{cl} = 1026\,°K$. With these conditions, we have $\theta_{cl} = 0{\cdot}1$ and the interaction parameter N may be calculated by equation (6) as 0·104. With these values of $N = 0{\cdot}104$ and $\theta_{cl} = 0{\cdot}1$, we then obtain $\xi' = 0{\cdot}55$ from Fig. 8, and the total heat flux is obtained from Fig. 9 as

$$Q_w^T = 0{\cdot}11$$

or

$$q_w^T = 49\,\text{cal/cm}^2\,\text{h (or } 180\,\text{Btu/ft}^2\,\text{h}).$$

Similarly, for the large path length limit, we may obtain analogous results concerning the heat-transfer process.

CONCLUDING REMARKS

Numerical results for the optically thin and large path length limit are obtained for the nongray gases H_2O, CH_4, CO_2 and CO flowing in a circular tube having a constant wall temperature. It is found that the optically thin approximation may be used for the calculation of heat transfer within reasonable accuracy when the dimensionless path length, u_0, is less than 0·4. For the large path length limit, no general criterion can be drawn for the applicability of this limit. The range of the optical thickness to apply the large path length limit approximation is different for different gases.

REFERENCES

1. C. S. Landram, R. Greif and I. S. Habib, Heat transfer in turbulent pipe flow with optically thin radiation, *J. Heat Transfer* **91**, 330–336 (1969).
2. I. S. Habib and R. Greif, Heat transfer to a flowing non-gray radiating gas: an experimental and theoretical study, *Int. J. Heat Mass Transfer* **13**, 1571–1581 (1970).
3. D. R. Jeng, E. J. Lee and K. J. DeWitt, Simultaneous conductive, convective and radiative heat transfer for laminar flow in circular tubes with constant wall temperature, *Proc.* 5th *Int. Heat Transfer Conf.* R2.12, Vol. 1, pp. 118–122. Am. Soc. (1974).
4. E. J. Lee, Heat transfer by thermal radiation in forced convective tube flow of a radiating gas, Ph.D. thesis, University of Toledo (1972).
5. C. L. Tien and J. E. Lowder, A correlation for total band absorption of radiating gases, *Int. J. Heat Mass Transfer* **9**, 698–701 (1966).
6. D. K. Edwards, L. K. Glassen, W. C. Hauser and J. S. Tuchscher, Radiation heat transfer in non-isothermal, non-gray gases, *J. Heat Transfer* **C89**, 219–228 (1967).

ETUDE DE DEUX CAS LIMITES DU TRANSFERT THERMIQUE PAR CONVECTION ET RAYONNEMENT DANS DES GAS NON-GRIS

Résumé—Une étude de transfert thermique par convection et rayonnement est effectuée pour deux limites optiques dans des gaz non-gris s'écoulant dans un tube circulaire avec température de paroi uniforme. Les équations fondamentales d'énergie, valables dans les deux limites des milieux optiquement minces et optiquement épais, sont obtenues pour l'écoulement laminaire établi avec une paroi non noire. On a obtenu des résultats numériques relatifs aux profils de température, aux flux locaux de conduction et de rayonnement et aux flux totaux; le domaine de validité de ces cas limites est discuté.

DIE UNTERSUCHUNG ZWEIER GRENZFÄLLE DES WÄRMEÜBERGANGS DURCH KONVEKTION UND STRAHLUNG IN NICHTGRAUEN GASEN

Zusammenfassung—Der Wärmeübergang durch Konvektion und Strahlung an nichtgraue Gase, die durch ein Rohr mit konstanter Wandtemperatur strömen, wird für zwei optische Grenzfälle untersucht. Die den Vorgang beschreibenden Energiegleichungen, die für die Grenzfälle der kleinen und großen optischen Weglängen gültig sind, werden für den Fall der voll ausgebildeten laminaren Strömung mit einer nichtschwarzen Wand aufgestellt. Für die Temperaturprofile, die örtlichen Wärmeströme durch Konvektion und Strahlung und die Gesamtwärmeströme werden numerische Ergebnisse angegeben. Die Gültigkeit der beiden Grenzfälle wird diskutiert.

ИССЛЕДОВАНИЕ ДВУХ ПРЕДЕЛЬНЫХ СЛУЧАЕВ КОНВЕКТИВНОГО И ЛУЧИСТОГО ПЕРЕНОСА ТЕПЛА В НЕСЕРЫХ ГАЗАХ

Аннотация — Исследуется два предельных случая конвективного и лучистого теплообмена несерых газов при течении в кольцевой трубе с постоянной однородной температурой стенки. Для случая полностью развитого ламинарного течения при наличии нечерной стенки выведены определяющие уравнения энергии, справедливые для предельных случаев оптически малых и больших длин пробега. Получены численные результаты для профилей температуры и локальных значений кондуктивного, лучистого и суммарного тепловых потоков и рассмотрена справедливость указанных предельных случаев.